HHS Public Access

Author manuscript

Neuroimage. Author manuscript; available in PMC 2017 July 01.

Published in final edited form as:

Neuroimage. 2016 July 1; 134: 122–131. doi:10.1016/j.neuroimage.2016.03.074.

Alpha power indexes task-related networks on large and small scales: a multimodal ECoG study in humans and a non-human primate

A. de Pesters[a,b], **W. G. Coon**[a], **P. Brunner**[a,c], **A. Gunduz**[d], **A. L. Ritaccio**[c], **N.M. Brunet**[e], **P. de Weerd**[f,g], **M.J. Roberts**[g], **R. Oostenveld**[g], **P. Fries**[g,h], and **G. Schalk**[a,b,c,*]

[a]Nat Ctr for Adapt Neurotech, Wadsworth Center, NY State Dept of Health, Albany, NY, USA [b]Dept of Biomed Sci, State Univ of New York at Albany, Albany, NY, USA [c]Dept of Neurology, Albany Medical College, Albany, NY, USA [d]Dept of Biomed Eng, Univ of Florida, Gainesville, FL, USA [e]SUNY Downstate Med Ctr, Brooklyn, NY, USA [f]Dept of Cogn Neurosci, Maastricht Univ, Maastricht, Netherlands [g]Donders Inst for Brain, Cognition and Behaviour, Nijmegen, Netherlands [h]Ernst Strüngmann Inst for Neurosci, Frankfurt, Germany

Abstract

Performing different tasks, such as generating motor movements or processing sensory input, requires the recruitment of specific networks of neuronal populations. Previous studies suggested that power variations in the alpha band (8–12 Hz) may implement such recruitment of task-specific populations by increasing cortical excitability in task-related areas while inhibiting population-level cortical activity in task-unrelated areas (Klimesch et al., 2007; Jensen and Mazaheri, 2010). However, the precise temporal and spatial relationships between the modulatory function implemented by alpha oscillations and population-level cortical activity remained undefined. Furthermore, while several studies suggested that alpha power indexes task-related populations across large and spatially separated cortical areas, it was largely unclear whether alpha power also differentially indexes smaller networks of task-related neuronal populations. Here we addressed these questions by investigating the temporal and spatial relationships of electrocorticographic (ECoG) power modulations in the alpha band and in the broadband gamma range (70–170 Hz, indexing population-level activity) during auditory and motor tasks in five human subjects and one macaque monkey. In line with previous research, our results confirm that broadband gamma power accurately tracks task-related behavior and that alpha power decreases in task-related areas. More importantly, they demonstrate that alpha power suppression lags population-level activity in auditory areas during the auditory task, but precedes it in motor areas during the motor task. This suppression of alpha power in task-related areas was accompanied by an increase in areas not related to the task. In addition, we show for the first time that these

*Corresponding author, Gerwin Schalk, Ph.D., National Center for Adaptive Neurotechnologies, Center for Medical Sciences 2003, 150 New Scotland Avenue, Albany, New York 12208, USA, gschalk@neurotechcenter.org.

differential modulations of alpha power could be observed not only across widely distributed systems (e.g., motor vs. auditory system), but also within the auditory system. Specifically, alpha power was suppressed in the locations within the auditory system that most robustly responded to particular sound stimuli. Altogether, our results provide experimental evidence for a mechanism that preferentially recruits task-related neuronal populations by increasing cortical excitability in task-related cortical areas and decreasing cortical excitability in task-unrelated areas. This mechanism is implemented by variations in alpha power and is common to humans and the non-human primate under study. These results contribute to an increasingly refined understanding of the mechanisms underlying the selection of the specific neuronal populations required for task execution.

Keywords

electrocorticography (ECoG); auditory processing; alpha oscillations; broadband gamma; information gating

1. Introduction

Performing different tasks, such as generating motor movements or processing sensory information, requires the recruitment of specific networks of neuronal populations dispersed throughout distinct cortical areas. How the brain implements the recruitment of these networks is still largely unclear, but there is increasing evidence that oscillatory activity plays an important role in this process. For example, several studies involving different sensorimotor modalities have reported a decrease in the power of low-frequency oscillations (event-related desynchronization (ERD)) in the 8–12 Hz range (alpha band) in task-related areas (Pfurtscheller and Neuper, 1992; Crone et al., 2001; Potes et al., 2014). This phenomenon is frequently coupled with an increase in alpha power (event-related synchronization (ERS)) in areas unrelated to the task (Pfurtscheller and Berghold, 1989; Pfurtscheller and Neuper, 1992; Fu et al., 2001). Separately, alpha oscillations with higher amplitudes modulate the firing of neuronal populations more strongly than oscillations with lower amplitudes (Haegens et al., 2011), which establishes a link between modulations of alpha power and cortical excitability. Taken together, these findings suggest that modulations in alpha power may index the degree of inhibition in different cortical areas, and, by extension, the spatial representation of selected functional networks (Klimesch et al., 2007). These observations have been consolidated into the *gating-by-inhibition* (GBI) hypothesis (Jensen and Mazaheri, 2010), and most recently synthesized with the *communication-through-coherence* (CTC) hypothesis (Fries, 2005)) into the *function-through-biased oscillations* (FBO) hypothesis (Schalk, 2015). The view that emerges from this theoretical and experimental work is that the selection of functional networks is achieved by modulation of cortical excitability, and that cortical excitability is measured most directly by the instantaneous amplitude of oscillatory activity (that is influenced by oscillatory phase as well as oscillatory power) (Schalk, 2015).

If oscillatory activity indeed provides a general mechanism for the selection of cortical networks through modulation of cortical excitability, we can make three specific predictions.

First, increases in population-level cortical activity in task-related areas should be accompanied by a decrease in alpha power irrespective of the task or the involved cortical areas, and alpha power should increase in all other regions. Second, in top-down preparation for a motor output, increases in cortical excitability as measured by a decrease of alpha power should occur prior to increases in population-level cortical activity. On the contrary, in a bottom-up response to a sensory stimulus, cortical excitability modulations may also be affected by the stimulus, and should thus trail stimulus-induced cortical activity. While the suppression in the alpha band has previously been reported to precede motor movements (Pfurtscheller and Berghold, 1989; Pfurtscheller and Neuper, 1992) and to follow auditory stimulation (Crone et al., 2001), such results remained to be demonstrated using single-trial analyses. Third, we should observe task-selective alpha modulations not only on large spatial scales, e.g., across motor and auditory regions, but also on smaller scales, e.g., within auditory regions. Such small-scale modulations of oscillatory activity are a prerequisite if they were to play a central role in regulating information flow within the brain. While there is solid evidence supporting the idea that alpha power may constitute a selection mechanism across large, spatially separated areas (Pfurtscheller, 1992; Pfurtscheller and Neuper, 1994; Foxe et al., 1998; Thut et al., 2006), evidence that it may also support selection of small and interwoven networks is scarce (Harvey et al., 2013). At present, the general consensus is still that modulations of alpha power are spatially widespread and only poorly informative of detailed delineations of the functional networks underlying the performance of different tasks (Crone et al., 2001; Pfurtscheller et al., 2003; Crone et al., 2006; Miller et al., 2009a).

To test these predictions and to better understand the dynamics between modulatory alpha band oscillations and population-level cortical activity, we recorded electrocorticographic signals (ECoG) during auditory and motor tasks in five human subjects and one macaque monkey. The high spatial and temporal resolution of these signals allowed us to study these dynamics not only across functional networks, i.e., auditory versus motor systems, but also within one functional network, i.e., the auditory system. In particular, we evaluated the spatial and temporal patterns of alpha power in response to different types of stimuli, over time, and in specific locations of auditory cortex, and related them to modulations of population-level activity as indexed by broadband gamma (70–170 Hz) (Manning et al., 2009; Miller et al., 2009b; Ray and Maunsell, 2011).

In agreement with the three predictions outlined above, we observed large modulations of alpha power across tasks: alpha power decreased in task-related areas and increased in a majority of task-unrelated areas. These results were common to the human subjects and the macaque monkey. Because alpha power has been linked to cortical excitability, these changes likely subserve the preferential recruitment of those functional networks necessary to perform a particular task. Furthermore, we found that alpha power suppression lagged population-level activity in auditory areas during the auditory task, but preceded it in the motor areas during the motor task. Finally, decreases in alpha power within auditory areas indexed regions where population-level activity increased the most in response to specific auditory stimuli. Similarly, increases in alpha power indexed regions where population-level activity increased the least. Taken together, our results add further evidence to a central role of oscillatory activity in regulating cortical excitability, and thus in regulating information

flow within the brain. They also suggest that this modulating mechanism might operate even across small cortical populations.

2. Methods

2.1. Subjects

Five human subjects at Albany Medical Center (Albany, New York) and one macaque monkey at Radboud University (Nijmegen, Netherlands) participated in this study. The five human subjects (A–E) were patients with intractable epilepsy who underwent temporary placement of subdural electrode arrays to localize seizure foci prior to surgical resection. They included two women (A and B) and three men (C, D and E). The subjects' clinical profiles is summarized in Table 1. Language lateralization (LL) was established preoperatively using the Wada test (Wada and Rasmussen, 1960). Human subjects gave informed consent for the study, which was approved by the Institutional Review Board of Albany Medical College and the Human Research Protections Office of the US Army Medical Research and Materiel Command. All animal procedures were approved by the ethics committee of Radboud University, Nijmegen, Netherlands.

The subjects were implanted with electrode grids that were approved for human use (Ad-Tech Medical Corp., Racine, WI; and PMT Corp., Chanhassen, MN; for human subjects), or polyimide-based grids (Rubehn et al., 2009, for the macaque) over one hemisphere of the brain. Electrodes for the humans consisted of platinum-iridium discs (4 mm in diameter, 2.3 mm exposed), embedded in silicon and spaced 6–10 mm apart; for the macaque, electrodes were 1 mm in diameter and spaced 2, 2.5 or 3 mm apart. The total numbers of implanted electrodes were 58–134 for the humans and 252 for the macaque. In the humans, the grids were implanted for about 1 week and their location varied across subjects. They were placed over the left hemisphere for subjects A, C, D, E and the macaque, and covered frontal, parietal and temporal cortices. Following the placement of the subdural grid, each human subject had postoperative anterior-posterior and lateral radiographs, as well as computer tomography (CT) scans to verify grid location.

2.2. Data Collection

We recorded ECoG signals from the five human subjects at the bedside using the general-purpose BCI2000 software (Schalk et al., 2004; Schalk and Mellinger, 2010) connected to eight 16-channel g.USBamp biosignal acquisition devices (g.tec, Graz, Austria). Clinical monitoring occurred simultaneously with the use of a connector that split the cables coming from the patient into one set that was connected to the clinical monitoring system and another set that was connected to the amplifiers. This ensured that clinical data collection was not compromised at any time. The signals were amplified, digitized at 1,200 Hz and stored by BCI2000. We used electrode contacts distant from epileptic foci and areas of interest for reference and ground. After visual inspection, we removed from all subsequent analyses those channels that did not contain clear ECoG signals (e.g., ground/reference channels, channels with broken connections, presence of environmental artifacts, or interictal activity). We also removed occipital channels to avoid any confound due to the visual presentation of instructions during the tasks. This left 56–121 channels for further

analyses. In addition to recording brain activity, we also simultaneously recorded the subjects' behavior using a push button.

We recorded and amplified ECoG signals from the macaque using eight 32-channel headstages (Plexon Headstage 32 V-G20). We low-pass filtered these signals at 8 kHz, digitized them at 32 kHz (Neuralynx Digital Lynx 256 channel system) and resampled them at 1,200 Hz. 229 channels remained for further analysis after visual inspection for the presence of artifacts.

2.3. Anatomical mapping

We created subject-specific 3D cortical brain models for subjects A, C, D and E using high-resolution pre-operative magnetic resonance imaging (MRI) scans and Curry software (Neuroscan Inc., El Paso, TX). MRI scans were not available for subject B. Instead, for visualization purposes, we used the 3D cortical template by the Montreal Neurological Institute (MNI)[1]. To identify the stereotactic coordinates of each grid electrode, we co-registered the MRI scans with post-operative computer tomography (CT) images. Finally, we projected each patient's electrode locations onto the corresponding 3D brain model and rendered activation maps using the NeuralAct software package (Kubanek and Schalk, 2014).

For the macaque, the assignment of electrodes to cortical areas was based on high-resolution intra-operative photographs taken before and after grid placement, and used primarily sulcal landmarks.

2.4. Tasks and stimuli

During the auditory task, the human subjects and the macaque passively listened to natural auditory stimuli while otherwise resting. The stimuli consisted of 19 natural sounds that belonged to one of six different categories: speech (female and male voices (3 stimuli)), music (classical and jazz (4)), nature (forest, thunderstorm, water and waves (4)), animals (frogs, birds and dog (5)), engines (jet airplane and train (2)), or white noise (1). Each stimulus had a duration of 10 seconds. Stimuli were digitized at 44.1 kHz in waveform audio file format, and energy-matched.

We presented the stimuli in 10 blocks. Each block contained a randomly interleaved sequence of the 19 stimuli. We used binaural in-ear earphones (12 to 23.5 kHz audio bandwidth, 20 dB isolation from environmental noise) for the human subjects and a loudspeaker for the macaque. The sound volume was adjusted to a comfortable level for each subject.

At the end of each stimulus, we verified the human subject's attention to the stimulus by engagement in a motor task in which s/he had to decide to which category the presented stimulus belonged. Specifically, two seconds after the end of the auditory stimulus presentation, we presented on a screen the names of two of the stimulus categories (e.g., 'speech', 'music'). The names were presented simultaneously and next to each other. One of

[1] http://www.bic.mni.mcgill.ca

the names was the category to which the last stimulus belonged; the other one was randomly chosen from the other categories. Subjects were asked to assign the last stimulus to one of the two categories by pressing one of two possible response keys (e.g., left button for the choice on the left or right button for the choice on the right). Subjects used the hand contralateral to the grid implantation for the button press. The stimulus presentation resumed after a 2-second interval. Results of the behavioral data indicated that the human subjects were attending to the auditory stimuli. They correctly categorized the stimuli with an average accuracy of 97 % (range: 92–99 %; accuracy due to chance: 50 %).

2.5. Feature extraction

To extract spectral power in the alpha and broadband gamma bands, we first high-pass filtered the signals at 0.1 Hz to remove drift. We then re-referenced the signals to a common average reference (CAR) montage for the human subjects and a bipolar montage for the macaque [2]. We band-pass filtered the signals in the two frequency bands of interest, i.e., 8–12 Hz (alpha) and 70–170 Hz (broadband gamma) using Butterworth filters of the same order for the two bands. Next, for each subject, location, and stimulus, we removed evoked components in the alpha band (Klimesch et al., 2007; Fujioka and Ross, 2008) by subtracting the amplitude of alpha averaged across trials from the individual trials, according to the inter–trial variance method proposed by Kalcher and Pfurtscheller in 1995. We then extracted amplitude envelopes by computing the absolute value of the Hilbert transform of the corresponding bandpass-filtered signals, followed by a low-pass Butterworth filter at 4 Hz and down-sampling to 120 Hz. Finally, we normalized the amplitude envelopes to a baseline period, i.e., a 300 ms period just prior to the onset of the auditory stimulus. We chose this baseline period as the longest period of time that did not contain significant changes of broadband gamma or alpha power between averaged trials after visual inspection. We used the same baseline for all analyses throughout the study. For the remainder of the manuscript, we will refer to the signals that we obtained with these procedures as alpha and broadband gamma power, respectively.

To extract the sound intensity of the auditory stimuli, we first computed the square root of the squared amplitude of each stimulus. Similar to the neural signals, we then low-pass filtered the resulting signal at 4 Hz and down-sampled it at 120 Hz.

2.6. Data analyses

2.6.1. Spatial analysis—We first determined which cortical locations were responsive to the auditory or motor tasks, i.e., which locations exhibited higher broadband gamma power during the task period when compared to the baseline time period. For the auditory task, we defined the task period as the first 500 ms of auditory stimulus presentation. For the motor task, we defined the task period as the period from −250 ms to +250 ms relative to the button press. For each location and each task, we separately concatenated the task and baseline samples across all trials. We then calculated the coefficient of determination (Spearman's r^2 value) between the baseline and task samples to determine the fraction of the total signal

[2]Data for the macaque were collected across several different data acquisition systems, which invalidates the calculation of a spatial average across all channels.

variance that was related to the task. We determined the statistical significance of these r^2 values using a permutation test in which we randomly reassigned the label (task or baseline) to each time period and calculated the corresponding random r^2 value. (Note that we did not shuffle the samples within each time period, so the auto-correlation of the signal was preserved.) We repeated the randomization step 1000 times, generating a distribution of random r^2 values. We considered an observed r^2 value to be significant at the 99th percentile of that distribution ($p < 0.01$, Bonferroni-corrected for the total number of electrodes in each subject). Our permutation test resulted in a set of reactive locations that defined task-related cortical areas, i.e., areas active during the auditory or motor task. Finally, we calculated the size of the observed effect at each location by computing the z-score obtained after normalizing the observed r^2 value against the mean and standard deviation of the random r^2 values distribution. The same process was applied to both the human and the macaque data [1].

To quantify the spatial changes of alpha power in response to the auditory and motor tasks, we first determined whether the distribution of alpha power onset responses at each location was different from 0. For the locations that displayed a significant difference (two-sided t-test, $p < 0.05$, Bonferroni corrected for the number of locations) we determined whether the difference was positive or negative using a one-sided t-test ($p < 0.05$). This resulted in 3 sets of locations that displayed either an increase, a decrease, or no change of alpha power, respectively. We then compared the distributions of percentages of locations displaying an alpha power increase or decrease for each task using a two-sided t-test ($p < 0.05$).

2.6.2. Temporal analyses—We first determined the temporal relationship between alpha and broadband gamma power, for each task period and across all the task-related locations previously defined. More specifically, we asked which of the two signals (i.e., alpha and broadband gamma) preceded the other in their modulations. To answer this question, we determined the delay between the positive peak of broadband gamma power and the negative peak of alpha power in single trials. We first low-pass filtered the power in the alpha and broadband gamma bands at 2 Hz (MATLAB filtfilt command for zero phase-lag filtering). Next, for each frequency band, we averaged the power across those locations that were reactive during a particular task (i.e., auditory or motor). For each trial, we then determined the time of the maximum amplitude in the broadband gamma signal, and minimum amplitude in the alpha signal. In this analysis, we used the 200 to 800 ms period after auditory stimulus onset in the auditory reactive locations, and the −300 to 300 ms period relative to the button press in the motor reactive locations. This resulted in one peak time per trial, task and each of the two frequency bands. From the 190 trials, we obtained a distribution for each task and frequency band. After removing outliers (<5th or >95th percentiles), we applied a two-sided paired t-test to determine which of the two bands (i.e., alpha or broadband gamma) preceded the other.

[1]Since the macaque did not use his hand to verify the auditory stimulus, we defined motor cortical locations using separately collected data involving controlled hand motor movements. These hand movements were highly variable in duration and movement speed. Thus, they did not allow us to calculate event-related motor responses in the macaque. In addition, in the macaque, we only considered those locations that were posterior to the central sulcus during the auditory task, or anterior to the central sulcus during the motor task.

To further establish the temporal relationship between alpha and broadband gamma power, we investigated whether the times of the peaks of the responses were related to each other. To do this, we computed the Spearman's correlation coefficients between the times of the negative and positive peaks of alpha and broadband gamma power, respectively.

2.6.3. Correlation analyses—We investigated how the moment-by-moment variations in alpha power, sound intensity and broadband gamma power relate to each other. Specifically, we quantified these relationships by computing the Spearman's correlation coefficient between alpha power and sound intensity, and between alpha power and broadband gamma power. In this context, it is important to recognize that each location will respond to the auditory stimulation with a different delay. To account for this delay, we temporally aligned the time course of alpha power with those of sound intensity and broadband gamma power. To do this, for each location, we first concatenated the signal time courses across all stimuli after averaging across repetitions. We then shifted the alpha time course by the delay (between 0 and 300 ms) that minimized the cross-correlation between alpha power and sound intensity/broadband gamma power. We then computed the Spearman's correlation coefficient r between alpha power and the sound intensity/broadband gamma power time courses for each location. To assess the statistical significance of the obtained observed correlation coefficient, we performed a permutation test in which we circularly shifted the reversed time course of alpha power by a random value and calculated the corresponding Spearman's correlation coefficient between the obtained time courses. We repeated this randomization step 500 times, generating a distribution of random r values. We considered an observed r value to be significant at the 95th percentile of that distribution ($p < 0.05$, Bonferroni-corrected for the number of auditory locations in each subject). Finally, for each subject, we computed the median delay and r^2 across locations displaying a significant correlation value, along with the percentages of those locations.

3. Results

3.1. Spatial distribution of broadband gamma activations

The locations that were reactive during the auditory and motor tasks for each subject are shown in Figure 1. In line with previous research, in the human subjects, we found these locations primarily close to superior temporal gyrus (STG) or other perisylvian regions during the auditory task (Crone et al., 2001; Edwards et al., 2009), and close to premotor, motor and somatosensory cortices during the motor task (Crone et al., 1998; Miller et al., 2007). Thus, these results confirm that task-related increases in broadband gamma power can robustly localize functional cortical areas (Brunner et al., 2009; Crone et al., 2011; Miller et al., 2014). In the macaque monkey, these locations were largely concentrated around STG during the auditory task and around primary motor cortex (F1), dorsal premotor area (F2) and ventral premotor area (F4) during the motor task.

3.2. Differential amplitude relationship of broadband gamma and alpha modulations across large-scale cortical systems

To approach the main questions posed in our study, we established the relationship of the amplitude of broadband gamma and alpha responses to the auditory and motor tasks, i.e.,

across two different large-scale cortical systems. According to our first prediction, we expected to locate decreased alpha power in task-related regions (identified by increased broadband gamma), and increased alpha power in task-unrelated regions. Our results confirm this prediction.

Figure 2 summarizes the average power in alpha and broadband gamma across all task-related locations during auditory or motor tasks, respectively (auditory task: 200 to 800 ms following auditory stimulus onset; motor task: −300 to 300 ms relative to the button press). These results show that in the auditory locations, the broadband gamma power increase during the auditory task was accompanied by a decrease in alpha power (two-sided t-test; see Figure 2 for significance values). Such induced depression of alpha power over the auditory cortex is consistent with previous studies reporting a decrease of the so-called tau rhythm centered around 10 Hz during the presentation of auditory stimuli (Tiihonen et al., 1991; Krause et al., 1994; Lehtelä et al., 1997). The same relationship was conserved in the motor locations during the motor task, where broadband gamma power increased and alpha power decreased (two-sided t-test; $p < 0.001$ for the humans). This finding is also consistent with the well-established event-related suppression of the mu rhythm (8–12 Hz) during motor movements (Pfurtscheller and Berghold, 1989).

These results also demonstrate that the reduction in alpha power in task-related areas was paralleled by an increase in alpha power in the task-related area of the opposite task (two-sided t-test; see Figure 2 for significance values). For example, during the auditory task, alpha power was increased in motor locations both in the human subjects (left panel) as well as the macaque (center panel).

Finally, we were interested whether this observed increase in alpha power would extend to cortical areas that were not involved in any of the two tasks investigated here. To provide a qualitative assessment, for each of the two tasks, we projected all the electrodes of the five human subjects or the macaque onto a three-dimensional template brain and rendered the color-coded alpha power during task onset at each location. The results are shown in Figure 3A–B. Results indicate that alpha power decreased in the corresponding reactive locations and increased over the majority of the cortical areas not involved in any of the tasks. Notably, we observed large increases in alpha power over the prefrontal and the inferior temporal cortices. In addition, the decrease in alpha power was spatially more restricted than the increase in alpha power (two-sided t-test, $p < 0.05$ for both tasks): 56 % of locations exhibited an increase in alpha power for the human subjects and 53 % for the macaque during the auditory task; and 60 % for the human subjects during the motor task (see Figure 3C). These results show that the increase in alpha power occurs in a majority of the locations.

3.3. Temporal relationship of broadband gamma and alpha modulations

We next determined whether the task-related decrease in alpha power preceded or followed the increase of population-level activity in the task-related locations. According to our second prediction, the task-related decrease in alpha power should lag the increase of population-level activity in the auditory locations during the auditory task, but precede it in the motor locations during the motor task. This would be in line with previous studies that

suggested that suppression in the alpha band follows auditory stimulation (Crone et al., 2001), while it precedes motor movements (Pfurtscheller and Berghold, 1989; Pfurtscheller and Neuper, 1992).

To qualitatively verify the temporal relationship between alpha power and population-level activity, we averaged the time traces of the power over all auditory or motor locations. The results for all subjects are shown in Figure 4 (see Figure S1 for individual human subjects' results). They indicate that, during the auditory task, broadband gamma power showed a clear onset response peaking at 230 ms, consistent with the times reported in other studies (161–250 ms range for Crone et al. 2001 and Edwards et al. 2009). This increase was followed by a decrease in the alpha band with a negative peak at 450 ms. This delay of about 200 ms between the broadband gamma and alpha power responses is consistent with the results observed in previous work (Edwards et al., 2009; Potes et al., 2014). During the motor task, a depression of alpha power peaked at 220 ms before the button press, during which the broadband gamma power reached its maximum. In sum, alpha power lagged broadband gamma power in auditory regions during the auditory task but preceded it in motor locations during the motor task.

We confirmed this temporal relationships of the peaks of these two signals in individual trials using quantitative statistical analyses (auditory task: two-sided paired t-test; $p < 0.001$ for the human subjects and the macaque; motor task: two-sided paired t-test; $p < 0.001$ for the human subjects). Furthermore, single-trial analyses established that the times of the negative and positive peaks of alpha and broadband gamma power, respectively, were significantly correlated for both auditory and motor tasks ($r = 0.23$ for the auditory task in the human subjects and $r = 0.49$ for the macaque; $r = 0.19$ for the motor task in the human subjects; $p < 0.001$ for each condition). These findings, consistent across all human subjects and the macaque, support our hypothesis that the central nervous system can regulate cortical excitability during top-down preparation for motor output and during bottom-up responses to an auditory stimulus. In both cases, alpha power modulations index these changes of cortical excitability.

3.4. Differential alpha modulations within the auditory system

Finally, if indeed oscillatory activity reflects a general mechanism that gates information flow throughout the cortex, similar task-related patterns of decrease and increase in alpha power should also be present within the small scale of a single cortical system (e.g., the auditory system).

Initial investigations suggested that this was the case. Specifically, while alpha power dropped consistently across the whole auditory system across all different types of auditory stimuli, alpha modulations in individual locations varied substantially across different types of stimuli. Figure 5 gives exemplary time course of alpha and broadband gamma power over the whole duration of the stimulus for two exemplary locations and four different exemplary stimuli in subject A.

We first investigated how the moment-by-moment variations in alpha power, sound intensity and broadband gamma power related to each other. The results of our correlation analyses

showed that alpha power was significantly negatively correlated with broadband gamma power in 69 ± 7 % of the auditory locations (mean $r^2 = 0.13$, $p < 0.05$, Bonferroni-corrected for the number of auditory locations in each subject), and was lagging it by a median of 160 ms. In contrast, alpha power was significantly negatively correlated with sound intensity in only 2 % of the auditory locations (mean $r^2 = 0.04$, $p < 0.05$, Bonferroni-corrected for the number of auditory locations in each subject), and lagged it by 170 ms. Because alpha power variations clearly trail broadband gamma power variations, our results suggest that during auditory stimulation, cortical excitability in the auditory locations is predominantly affected by variations in population-level cortical activity rather than variations in stimulus intensity.

To further quantify these modulations of broadband gamma and alpha power, we first sought to determine whether the alpha power decrease in response to each sound affected all locations within the auditory system or was instead limited to a subset of auditory locations. Hence, we computed the percentage of locations that displayed any type of change (i.e., increase or decrease) of alpha power during the auditory stimulation when compared to baseline. To do this, we first concatenated the whole alpha power time courses for stimuli of each category. We then computed the significance of a two-sided t-test on the obtained distributions ($p < 0.05$ Bonferroni corrected for the number of locations). We averaged across subjects the percentages of locations displaying a significant change of alpha power. This revealed that 91 ± 4 % of auditory locations displayed a significant change of alpha power in response to auditory stimulation.

We then investigated how these changes varied with categories. When broken down across the 6 different sound categories, we observed that 68 ± 15 % locations responded with a decrease of alpha power to speech stimuli, 58 ± 12 % to music stimuli, 48 ± 31 % to animal sounds, 35 ± 25 % to engine sounds, 25 ± 23 % to nature stimuli and 21 ± 22 % to the white noise stimulus (onesided t-test, $p < 0.05$ Bonferroni corrected for the number of locations and sound categories). Bar plots displaying the percentages of locations with a decrease, increase or non-significant change of alpha power for each sound category are presented in Figure S2.

Next, we identified the locations within the auditory system that responded the most or the least to each particular auditory stimulus. To do this, we averaged the broadband gamma power of each stimulus across trials and time, which yielded one value for each auditory location, subject and stimulus. In each subject and for each stimulus, we identified those locations whose broadband gamma power was within the top and bottom 25% of these distributions (i.e., the most and least reactive auditory locations, respectively). In summary, this procedure identified the sets of locations that responded the most or the least to a particular stimulus. These reactive locations were largely different across stimuli; on average, only 30% of the most reactive locations were common across a pair of stimuli. Finally, we averaged the broadband gamma and alpha power across the most or least reactive locations and across all stimuli and human subjects. Results for human subjects are shown in Figure 6. Notably, the alpha power decreased in the most reactive locations (two-sided t-test; $p < 0.001$), and was increased in the least reactive locations (two-sided t-test; $p < 0.05$), mirroring the increase versus decrease of alpha power previously observed across the auditory and motor systems. In the macaque, alpha power was higher than baseline in both

the least and most reactive locations, which may be attributed to the lack of sustained attention to the auditory stimulus.

Finally, we determined whether these dynamics were also present on a single-stimulus basis. To do this, we determined, for each stimulus, whether the alpha power in the least reactive locations was indeed larger than the alpha power in the most reactive locations: we averaged alpha power across trials, time and the least or most reactive locations for each stimulus and subject. This resulted in two distributions (i.e., one for the most reactive locations and one for the least reactive locations), where each data point represented the alpha power for one stimulus and one subject. A paired t-test between these two distributions revealed that alpha power in the least reactive locations was indeed robustly larger than in the most reactive locations on a single-stimulus basis (paired t-test, $p < 0.001$).

4. Discussion

4.1. Summary of results

In this study, we investigated the spatial and temporal dynamics of alpha and broadband gamma power modulation across two distinct systems (auditory and motor) and within the auditory system in both humans and one non-human primate. Our results confirm results from previous studies that showed increased broadband gamma power and decreased alpha power in task-related areas (Crone et al., 2001; Miller et al., 2007; Edwards et al., 2009; Potes et al., 2014). More importantly, our results demonstrated increased alpha power in task-unrelated areas, both across but also within large-scale cortical systems. In addition, the decrease in alpha power in the motor locations preceded gamma increases during the motor movement, but followed it in the auditory locations during the auditory task.

In sum, the results shown in this paper further highlight the critical role of oscillatory modulations in facilitating or inhibiting task-related processing, even within interwoven and spatially restricted networks.

4.2. Population-level activity, cortical excitability and the selection of functional networks

Throughout the study, we used modulations of broadband gamma power as a measure of population-level cortical activity. In contrast to the alpha band (8–12 Hz) and the canonical gamma band (30–60 Hz, Fries 2005; Engel et al. 2001), broadband gamma is widely believed not to be an oscillatory phenomenon. Several studies have demonstrated that modulations in broadband gamma power strongly correlate with the asynchronous firing of neuronal populations in humans (Manning et al., 2009) and non-human primates (Whittingstall and Logothetis, 2009; Ray and Maunsell, 2011). As such, broadband gamma is a direct and robust measure of population-level activity levels that is related to the average firing rate of populations of neurons directly underneath the recording electrode. It should be noted that the frequency range that we considered in our study (70–170 Hz) is a sufficient approximation of the wider broadband signal reported by Miller et al. (Miller, 2010; Miller et al., 2014), which is not theoretically limited by any cutoff frequencies except for the ones imposed by the noise-floor of the recording device and the sampling rate of the recording (Miller et al., 2009b).

Over the last decade and increasingly during the last few years, several ECoG studies have demonstrated that broadband gamma power specifically increases in task-related locations. Such results have been obtained during a large variety of tasks, such as auditory perception (Crone et al., 2001; Canolty et al., 2007; Edwards et al., 2009; Potes et al., 2012), motor movements (Crone et al., 1998; Miller et al., 2007), visual spatial attention (Gunduz et al., 2011, 2012), auditory attention (Golumbic et al., 2013; Mesgarani and Chang, 2012; Dijkstra et al., 2015) or imagined speech (Pei et al., 2011a,b). Here, we used the broadband gamma response to locate areas that responded to the auditory and motor tasks. Our set of selected locations in the humans and the macaque monkey were in line with expectations based on prior studies investigating auditory processing (Crone et al. 2001; Edwards et al. 2009, for results in humans; Hackett et al. 1998; Rauschecker et al. 1995, for results in the macaque) and motor movements (Crone et al. 1998; Miller et al. 2007, for results in humans; Rizzolatti et al. 1998, for results in the macaque). Moreover, the locations in the humans co-localized with the hemodynamic responses observed during fMRI studies investigating complex sound processing (Mukamel et al., 2005) and hand movement (Lotze et al., 1999). Within the auditory network, we found that the responses in broadband gamma power during the auditory task were strongly specific to the type of auditory stimulus presented. Such specificity is in agreement with the compartmentalized representation of the auditory cortex derived from single-neuron studies in non-human primates (Rauschecker et al., 1995; Wang et al., 2005) and ECoG and fMRI studies in humans (Crone et al., 2001; Staeren et al., 2009; Leaver and Rauschecker, 2010). Taken together, these results support the view that increased broadband gamma power can accurately be used as an index of increased population-level activity and of task-related functional cortical networks.

In contrast, we found that the power in the alpha band consistently decreased over those same task-related areas and increased in task-unrelated areas, both across and within cortical systems. While the physiological origin of alpha oscillations has not yet been fully elucidated, it is well accepted that alpha power decreases with increased population-level activity, as demonstrated by its negative correlation with broadband gamma power (Crone et al., 2001; Miller et al., 2009a; Potes et al., 2014) and the blood-oxygen-level dependent (BOLD) response (Mukamel et al., 2005). The mechanisms supporting these apparent interrelationships between alpha and broadband gamma power are still unclear (but see Podvalny et al. 2015; Voytek et al. 2015; Voytek and Knight 2015). At the same time, alpha power decreases are clearly not simply a direct reflection of population-level activity since alpha power decreases can be observed in the absence of population-level activity and in preparation for an upcoming stimulus (Romei et al., 2010; Mazaheri et al., 2014). Hence, decreased oscillatory power is more likely an index of increased cortical excitability (i.e., an increased probability of cortical excitation) rather than a direct reflection of actual cortical excitation (Klimesch et al., 2007; Romei et al., 2008; Sauseng et al., 2009; Rajagovindan and Ding, 2011).

Conversely, an increase in alpha power is associated with a decrease of cortical excitability (Romei et al., 2008; Sauseng et al., 2009). Long considered a simple passive idling state (Adrian and Matthews, 1934; Pfurtscheller et al., 1996), alpha oscillations have more recently been shown to modulate population-level activity in a time-specific manner, with lower broadband gamma power (Osipova et al., 2008; Voytek et al., 2010) or lower firing

rates (Haegens et al., 2011) coinciding with the peaks of the alpha wave. Moreover, studies have demonstrated that increases in alpha power are not simply caused by a return to baseline from previously active cortical areas (Fu et al., 2001; Kelly et al., 2006). Therefore, increased alpha power has been considered to reflect an active inhibition phenomenon involved in the gating of cortical information (Klimesch et al., 2007; Jensen and Mazaheri, 2010).

The high spatial resolution of alpha power modulations that we observed within the auditory system in our study opposes the common notion that alpha oscillations are spatially widespread (Crone et al., 2001; Pfurtscheller et al., 2003; Crone et al., 2006; Miller et al., 2009a). Interestingly, most auditory studies investigating broadband gamma and alpha modulations employ short stimuli (Crone et al., 2001; Edwards et al., 2005, 2009), while the stimuli employed in the current study were 10 seconds long. It is possible that the stimulus specificity of alpha power modulations during sustained auditory stimulation changes over time, as has been demonstrated in previous studies (Picton et al., 1978a,b).

4.3. Current experimental limitations

As is the case with practically all human ECoG studies, the location of the electrode grids implanted in the five human subjects was dictated solely by clinical requirements. Thus, electrode coverage was variable across subjects, and limited to a single hemisphere. Furthermore, the clinical and cognitive state of the subjects is usually variable, both across but also within subjects over time, and can be influenced by their post-operative treatment plan and associated factors such as medication regimen or quality of sleep. At the same time, our behavioral validation indicated that all patients were able to meet the demands of the task and attend to the auditory stimuli. In addition, our results were consistent with the findings from other imaging modalities. Finally, definitively establishing the generalization of our results to macaques would require data collection in more macaque subjects.

5. Conclusion

In summary, the results of our study showed that alpha power is decreased in task-related areas and increased in task unrelated areas, both across but also within large-scale cortical systems. We also showed that alpha power decreases lag gamma power increases in the auditory system during an auditory task, but precede gamma power in the motor system during a motor task. We conclude that our results further strengthen the view that oscillatory activity shapes task-related cortical networks by differentially biasing cortical excitability. Our results suggest that this mechanism might operate not only across but also within large-scale functional networks, and may be conserved across species. Future research could further determine the generality of this mechanism, establish the causal role of oscillatory activity in this process, and delineate both the origin of oscillatory activity as well as its guiding parameters.

Supplementary Material

Refer to Web version on PubMed Central for supplementary material.

Acknowledgments

This work was supported by the NIH (EB00856, EB006356 and EB018783), the US Army Research Office (W911NF-08-1-0216, W911NF-12-1-0109, W911NF-14-1-0440) and Fondazione Neurone, the Netherlands organization for scientific research (VICI grant 453-04-002 to P.D.W. and VENI 451-09-025 to M.J.R.), and the Smart Mix Program of the Netherlands Ministry of Economic Affairs and the Netherlands Ministry of Education, Culture, and Science (BrainGain to R.O. and P.F.).

References

Adrian ED, Matthews BH. The Berger rhythm: potential changes from the occipital lobes in man. Brain. 1934; 57(4):355–385.

Brunner P, Ritaccio AL, Lynch TM, Emrich JF, Wilson JA, Williams JC, Aarnoutse EJ, Ramsey NF, Leuthardt EC, Bischof H, Schalk G. A practical procedure for real-time functional mapping of eloquent cortex using electrocorticographic signals in humans. Epilepsy Behav. 2009 Jul; 15(3): 278–286. [PubMed: 19366638]

Canolty RT, Soltani M, Dalal SS, Edwards E, Dronkers NF, Nagarajan SS, Kirsch HE, Barbaro NM, Knight RT. Spatiotemporal dynamics of word processing in the human brain. Front Neurosci. 2007; 1(1):185. [PubMed: 18982128]

Crone NE, Boatman D, Gordon B, Hao L. Induced electrocorticographic gamma activity during auditory perception. J Clin Neurophysiol. 2001 Apr; 112(4):565–582.

Crone NE, Korzeniewska A, Franaszczuk PJ. Cortical gamma responses: searching high and low. Int J Psychophysiol. 2011; 79(1):9–15. [PubMed: 21081143]

Crone NE, Miglioretti DL, Gordon B, Sieracki JM, Wilson MT, Uematsu S, Lesser RP. Functional mapping of human sensorimotor cortex with electrocorticographic spectral analysis. I. Alpha and beta event-related desynchronization. Brain. 1998 Dec; 121(Pt 12):2271–2299. [PubMed: 9874480]

Crone NE, Sinai A, Korzeniewska A. High-frequency gamma oscillations and human brain mapping with electrocorticography. Prog Brain Res. 2006; 159:275–295. [PubMed: 17071238]

Dijkstra K, Brunner P, Gunduz A, Coon W, Ritaccio A, Farquhar J, Schalk G. Identifying the attended speaker using electrocorticographic (ecog) signals. Brain-Computer Interfaces (ahead-of-print). 2015:1–13.

Edwards E, Soltani M, Deouell LY, Berger MS, Knight RT. High gamma activity in response to deviant auditory stimuli recorded directly from human cortex. J Neurophysiol. 2005; 94(6):4269–4280. [PubMed: 16093343]

Edwards E, Soltani M, Kim W, Dalal SS, Nagarajan SS, Berger MS, Knight RT. Comparison of ime-frequency responses and the event-related potential to auditory speech stimuli in human cortex. J Neurophys-iol. 2009; 102(1):377–386.

Engel AK, Fries P, Singer W. Dynamic predictions: oscillations and synchrony in top-down processing. Nat Rev Neurosci. 2001 Oct; 2(10):704–716. [PubMed: 11584308]

Foxe JJ, Simpson GV, Ahlfors SP. Parieto-occipital approximately 10 Hz activity reflects anticipatory state of visual attention mechanisms. Neuroreport. 1998; 9(17):3929–3933. [PubMed: 9875731]

Fries P. A mechanism for cognitive dynamics: neuronal communication through neuronal coherence. Trends Cogn Sci. 2005 Oct; 9(10):474–480. [PubMed: 16150631]

Fu K-MG, Foxe JJ, Murray MM, Higgins BA, Javitt DC, Schroeder CE. Attention-dependent suppression of distracter visual input can be cross-modally cued as indexed by anticipatory parieto-occipital alpha-band oscillations. Cognitive Brain Res. 2001; 12(1):145–152.

Fujioka T, Ross B. Auditory processing indexed by stimulus-induced alpha desynchronization in children. Int J Psychophysiol. 2008; 68(2):130–140. [PubMed: 18331761]

Golumbic EMZ, Ding N, Bickel S, Lakatos P, Schevon CA, McKhann GM, Goodman RR, Emerson R, Mehta AD, Simon JZ, et al. Mechanisms underlying selective neuronal tracking of attended speech at a cocktail party. Neuron. 2013; 77(5):980–991. [PubMed: 23473326]

Gunduz A, Brunner P, Daitch A, Leuthardt EC, Ritaccio AL, Pesaran B, Schalk G. Neural correlates of visual–spatial attention in electrocorticographic signals in humans. Front Hum Neurosci. 2011; 5:89. [PubMed: 22046153]

Gunduz A, Brunner P, Daitch A, Leuthardt EC, Ritaccio AL, Pesaran B, Schalk G. Decoding covert spatial attention using electrocorticographic (ECoG) signals in humans. NeuroImage. 2012; 60(4): 2285–2293. [PubMed: 22366333]

Hackett T, Stepniewska I, Kaas J. Subdivisions of auditory cortex and ipsilateral cortical connections of the parabelt auditory cortex in macaque monkeys. J Comp Neurol. 1998; 394(4):475–495. [PubMed: 9590556]

Haegens S, Nácher V, Luna R, Romo R, Jensen O. α-oscillations in the monkey sensorimotor network influence discrimination performance by rhythmical inhibition of neuronal spiking. P Natl Acad Sci USA. 2011; 108(48):19377–19382.

Harvey BM, Vansteensel MJ, Ferrier CH, Petridou N, Zuiderbaan W, Aarnoutse EJ, Bleichner MG, Dijkerman H, van Zandvoort MJ, Leijten F, et al. Frequency specific spatial interactions in human electrocorticography: V1 alpha oscillations reflect surround suppression. NeuroImage. 2013; 65:424–432. [PubMed: 23085107]

Jensen O, Mazaheri A. Shaping functional architecture by oscillatory alpha activity: gating by inhibition. Front Hum Neurosci. 2010:4. [PubMed: 20198130]

Kalcher J, Pfurtscheller G. Discrimination between phase-locked and non-phase-locked event-related EEG activity. Electroen Clin Neuro. 1995; 94(5):381–384.

Kelly SP, Lalor EC, Reilly RB, Foxe JJ. Increases in alpha oscillatory power reflect an active retinotopic mechanism for distracter suppression during sustained visuospatial attention. J Neurophysiol. 2006; 95(6):3844–3851. [PubMed: 16571739]

Klimesch W, Sauseng P, Hanslmayr S. EEG alpha oscillations: the inhibition-timing hypothesis. Brain Res Rev. 2007; 53(1):63–88. [PubMed: 16887192]

Krause CM, Lang HA, Laine M, Helle SI, Kuusisto MJ, Pörn B. Event-related desynchronization evoked by auditory stimuli. Brain Topogr. 1994; 7(2):107–112. [PubMed: 7696087]

Kubanek J, Schalk G. NeuralAct: A tool to visualize electrocortical (ECoG) activity on a three-dimensional model of the cortex. Neuroinformatics. 2014:1–8. [PubMed: 24174261]

Leaver AM, Rauschecker JP. Cortical representation of natural complex sounds: effects of acoustic features and auditory object category. J Neurosci. 2010; 30(22):7604–7612. [PubMed: 20519535]

Lehtelaä L, Salmelin R, Hari R. Evidence for reactive magnetic 10-Hz rhythm in the human auditory cortex. Neurosci Lett. 1997; 222(2):111–114. [PubMed: 9111741]

Lotze M, Montoya P, Erb M, Hülsmann E, Flor H, Klose U, Birbaumer N, Grodd W. Activation of cortical and cerebellar motor areas during executed and imagined hand movements: an fMRI study. J Cognitive Neurosci. 1999; 11(5):491–501.

Manning JR, Jacobs J, Fried I, Kahana MJ. Broadband shifts in local field potential power spectra are correlated with single-neuron spiking in humans. J Neurosci. 2009; 29(43):13613–13620. [PubMed: 19864573]

Mazaheri A, van Schouwenburg MR, Dimitrijevic A, Denys D, Cools R, Jensen O. Region-specific modulations in oscillatory alpha activity serve to facilitate processing in the visual and auditory modalities. Neu-roImage. 2014; 87:356–362.

Mesgarani N, Chang EF. Selective cortical representation of attended speaker in multi-talker speech perception. Nature. 2012 Apr; 485(7397):233–236. [PubMed: 22522927]

Miller K, Zanos S, Fetz E, Den Nijs M, Ojemann J. Decoupling the cortical power spectrum reveals real-time representation of individual finger movements in humans. J Neurosci. 2009a; 29(10): 3132–3137. [PubMed: 19279250]

Miller KJ. Broadband spectral change: evidence for a macroscale correlate of population firing rate? J Neurosci. 2010; 30(19):6477–6479. [PubMed: 20463210]

Miller KJ, Honey CJ, Hermes D, Rao RP, denNijs M, Ojemann JG. Broadband changes in the cortical surface potential track activation of functionally diverse neuronal populations. NeuroImage. 2014; 85:711–720. [PubMed: 24018305]

Miller KJ, Leuthardt EC, Schalk G, Rao RP, Anderson NR, Moran DW, Miller JW, Ojemann JG. Spectral changes in cortical surface potentials during motor movement. J Neurosci. 2007 Feb; 27(9):2424–2432. [PubMed: 17329441]

Miller KJ, Sorensen LB, Ojemann JG, Den Nijs M. Power-law scaling in the brain surface electric potential. PLoS Comp Biol. 2009b; 5(12):e1000609.

Mukamel R, Gelbard H, Arieli A, Hasson U, Fried I, Malach R. Coupling between neuronal firing, field potentials, and fMRI in human auditory cortex. Science. 2005 Aug; 309(5736):951–954. [PubMed: 16081741]

Osipova D, Hermes D, Jensen O. Gamma power is phase-locked to posterior alpha activity. PLoS One. 2008; 3(12):e3990. [PubMed: 19098986]

Pei X, Barbour DL, Leuthardt EC, Schalk G. Decoding vowels and consonants in spoken and imagined words using electrocorticographic signals in humans. J Neural Eng. 2011a; 8(4):046028. [PubMed: 21750369]

Pei X, Leuthardt EC, Gaona CM, Brunner P, Wolpaw JR, Schalk G. Spatiotemporal dynamics of electrocorticographic high gamma activity during overt and covert word repetition. NeuroImage. 2011b; 54(4):2960–2972. [PubMed: 21029784]

Pfurtscheller G. Event-related synchronization (ERS): an electrophysiological correlate of cortical areas at rest. Electroencephalogr Clin Neurophysiol. 1992; 83(1):62–69. [PubMed: 1376667]

Pfurtscheller G, Berghold A. Patterns of cortical activation during planning of voluntary movement. Clin Neurophysiol. 1989; 72:250–258.

Pfurtscheller G, Graimann B, Huggins JE, Levine SP, Schuh LA. Spatiotemporal patterns of beta desynchronization and gamma synchronization in corticographic data during self-paced movement. Clin Neuro-physiol. 2003; 114(7):1226–1236.

Pfurtscheller G, Neuper C. Simultaneous EEG 10 Hz desynchronization and 40 Hz synchronization during finger movements. Neuroreport. 1992; 3(12):1057–1060. [PubMed: 1493217]

Pfurtscheller G, Neuper C. Event-related synchronization of mu rhythm in the EEG over the cortical hand area in man. Neurosci Lett. 1994; 174(1):93–96. [PubMed: 7970165]

Pfurtscheller G, Stancak A Jr, Neuper C. Event-related synchronization (ERS) in the alpha band - an elec-trophysiological correlate of cortical idling: a review. Int J Psychophysiol. 1996; 24(1):39–46. [PubMed: 8978434]

Picton TW, Woods D, Proulx G. Human auditory sustained potentials. I. The nature of the response. Electroencephalogr Clin Neurophysiol. 1978a; 45(2):186–197. [PubMed: 78829]

Picton TW, Woods D, Proulx G. Human auditory sustained potentials. II. Stimulus relationships. Electroencephalogr Clin Neurophysiol. 1978b; 45(2):198–210.

Podvalny E, Noy N, Harel M, Bickel S, Chechik G, Schroeder CE, Mehta AD, Tsodyks M, Malach R. A unifying principle underlying the extracellular field potential spectral responses in the human cortex. Journal of neurophysiology. 2015; 114(1):505–519. [PubMed: 25855698]

Potes C, Brunner P, Gunduz A, Knight RT, Schalk G. Spatial and temporal relationships of electrocorticographic alpha and gamma activity during auditory processing. NeuroImage. 2014 Apr.

Potes C, Gunduz A, Brunner P, Schalk G. Dynamics of electrocorticographic (ECoG) activity in human temporal and frontal cortical areas during music listening. NeuroImage. 2012 Jul; 61(4): 841–848. [PubMed: 22537600]

Rajagovindan R, Ding M. From prestimulus alpha oscillation to visual-evoked response: an inverted-U function and its attentional modulation. J Cognitive Neurosci. 2011; 23(6):1379–1394.

Rauschecker JP, Tian B, Hauser M. Processing of complex sounds in the macaque nonprimary auditory cortex. Science. 1995; 268(5207):111–114. [PubMed: 7701330]

Ray S, Maunsell JH. Different origins of gamma rhythm and high-gamma activity in macaque visual cortex. PLoS Biol. 2011; 9(4):e1000610. [PubMed: 21532743]

Rizzolatti G, Luppino G, Matelli M. The organization of the cortical motor system: new concepts. Electroen Clin Neuro. 1998; 106(4):283–296.

Romei V, Brodbeck V, Michel C, Amedi A, Pascual-Leone A, Thut G. Spontaneous fluctuations in posterior α-band EEG activity reflect variability in excitability of human visual areas. Cereb Cortex. 2008; 18(9):2010–2018. [PubMed: 18093905]

Romei V, Gross J, Thut G. On the role of prestimulus alpha rhythms over occipito-parietal areas in visual input regulation: correlation or causation? J Neurosci. 2010; 30(25):8692–8697. [PubMed: 20573914]

Rubehn B, Bosman C, Oostenveld R, Fries P, Stieglitz T. A MEMS-based flexible multichannel ECoG-electrode array. J Neural Eng. 2009; 6(3):036003. [PubMed: 19436080]

Sauseng P, Klimesch W, Heise KF, Gruber WR, Holz E, Karim AA, Glennon M, Gerloff C, Birbaumer N, Hummel FC. Brain oscillatory substrates of visual short-term memory capacity. Curr Biol. 2009; 19(21):1846–1852. [PubMed: 19913428]

Schalk G. A general framework for dynamic cortical function: the function-through-biased-oscillations (FBO) hypothesis. Frontiers in Human Neuroscience. 2015; 9:352. [PubMed: 26136676]

Schalk G, McFarland DJ, Hinterberger T, Birbaumer N, Wolpaw JR. BCI2000: a general-purpose brain-computer interface (BCI) system. IEEE Trans Biomed Eng. 2004 Jun; 51(6):1034–1043. [PubMed: 15188875]

Schalk, G.; Mellinger, J. A Practical Guide to Brain–Computer Interfacing with BCI2000. Springer; 2010.

Staeren N, Renvall H, De Martino F, Goebel R, Formisano E. Sound categories are represented as distributed patterns in the human auditory cortex. Curr Biol. 2009; 19(6):498–502. [PubMed: 19268594]

Thut G, Nietzel A, Brandt SA, Pascual-Leone A. α-band electroencephalographic activity over occipital cortex indexes visuospatial attention bias and predicts visual target detection. J Neurosci. 2006; 26(37):9494–9502. [PubMed: 16971533]

Tiihonen J, Hari R, Kajola M, Karhu J, Ahlfors S, Tissari S. Magnetoencephalographic 10-Hz rhythm from the human auditory cortex. Neurosci Lett. 1991; 129(2):303–305. [PubMed: 1745412]

Voytek B, Canolty RT, Shestyuk A, Crone NE, Parvizi J, Knight RT. Shifts in gamma phase–amplitude coupling frequency from theta to alpha over posterior cortex during visual tasks. Front Hum Neurosci. 2010:4. [PubMed: 20198130]

Voytek B, Knight RT. Dynamic network communication as a unifying neural basis for cognition, development, aging, and disease. Biological psychiatry. 2015; 77(12):1089–1097. [PubMed: 26005114]

Voytek B, Kramer MA, Case J, Lepage KQ, Tempesta ZR, Knight RT, Gazzaley A. Age-related changes in 1/f neural electrophysiological noise. The Journal of Neuroscience. 2015; 35(38): 13257–13265. [PubMed: 26400953]

Wada J, Rasmussen T. Intracarotid injection of sodium amytal for the lateralization of cerebral speech dominance. J Neurosurg. 1960; 17:266–282.

Wang X, Lu T, Snider RK, Liang L. Sustained firing in auditory cortex evoked by preferred stimuli. Nature. 2005; 435(7040):341–346. [PubMed: 15902257]

Whittingstall K, Logothetis NK. Frequency-band coupling in surface EEG reflects spiking activity in monkey visual cortex. Neuron. 2009; 64(2):281–289. [PubMed: 19874794]

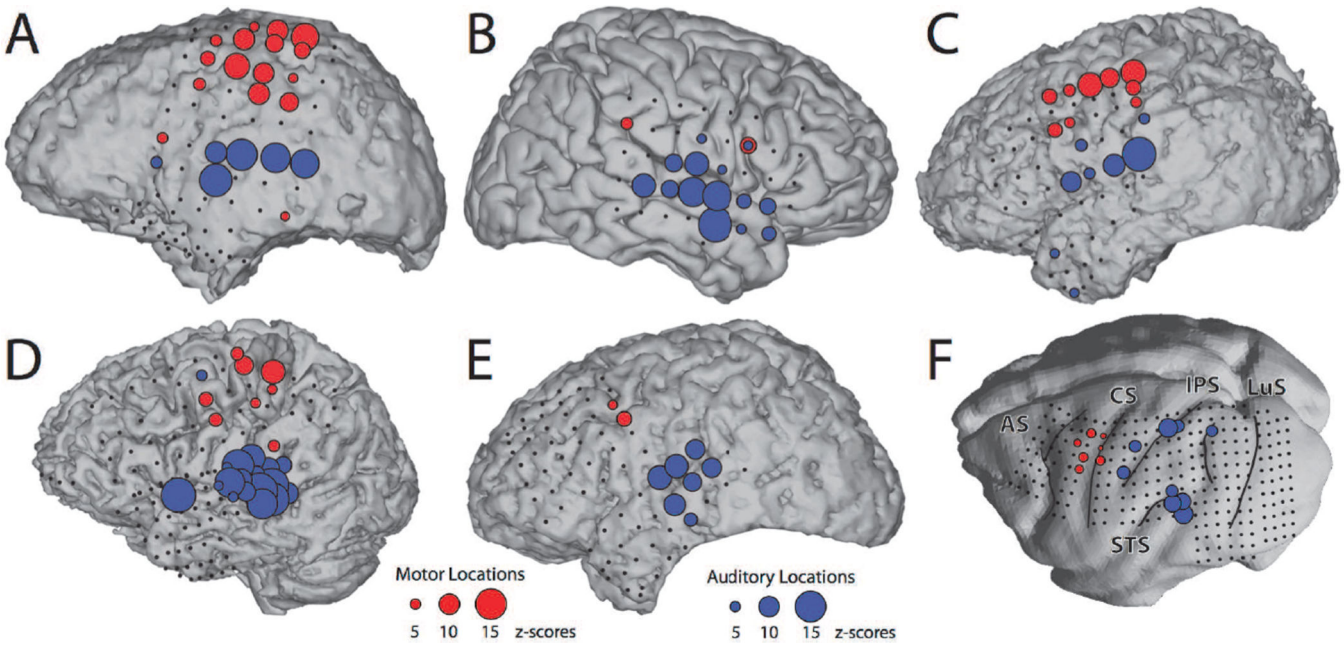

Figure 1. Increases in broadband gamma power index functional cortical locations

For each of the human subjects (**A–E**) and the macaque monkey (**F**), colored circles represent locations that were reactive during the auditory task (blue circles) or motor task (red circles). The size of the circle corresponds to the size of the response (see reference circles at the bottom of the figure). Small black circles denote non-reactive locations. They do not include artifactual and occipital electrodes that were removed from the analysis. AS, arcuate sulcus; CS, central sulcus; IPS, intraparietal sulcus; LuS, lunate sulcus; STS, superior temporal sulcus.

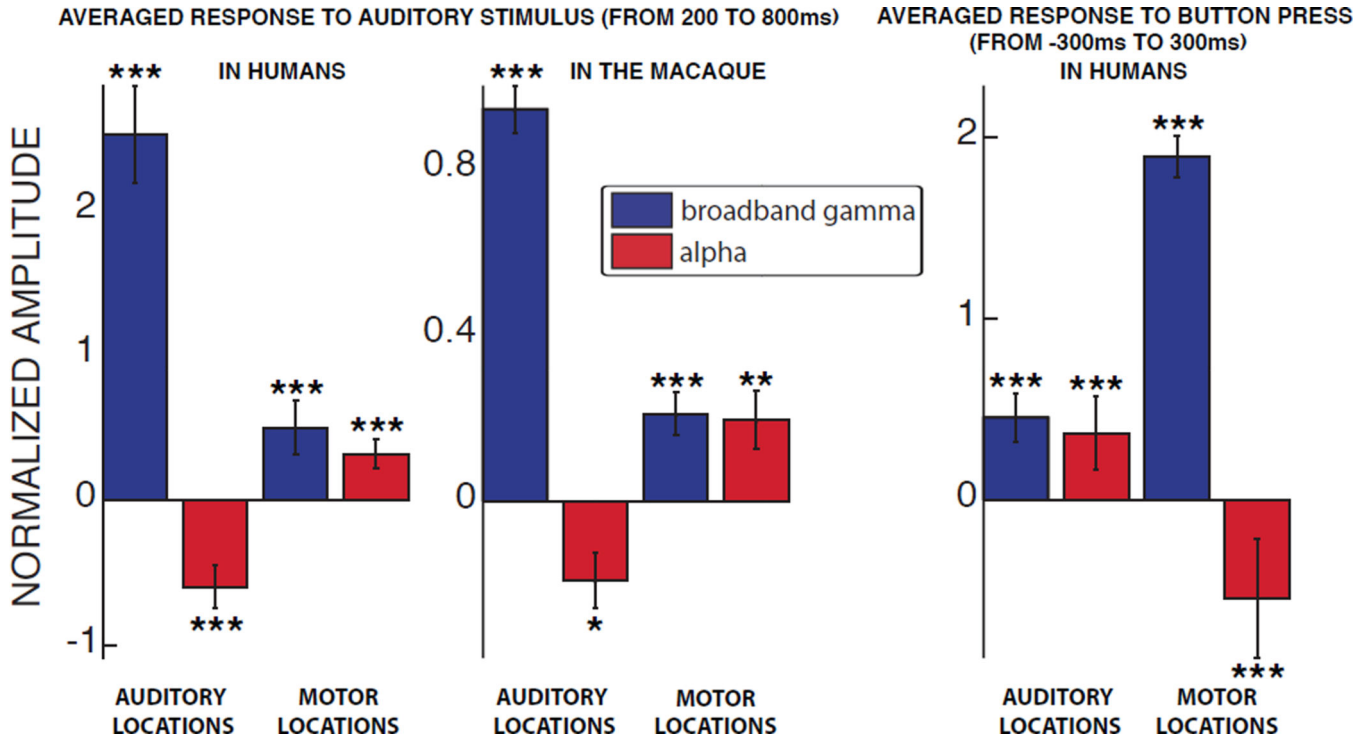

Figure 2. Alpha power is suppressed in task-related locations and increased in non-related locations

The bar plots show the amplitude of the responses, averaged across all task-related locations (i.e., auditory or motor areas), during the auditory task in humans (left panel), macaque (middle panel), and motor task in humans (right panel) for broadband gamma (blue) and alpha (red) bands. Error bars denote the standard error. *: $p < 0.05$; **: $p < 0.01$; ***: $p < 0.001$.

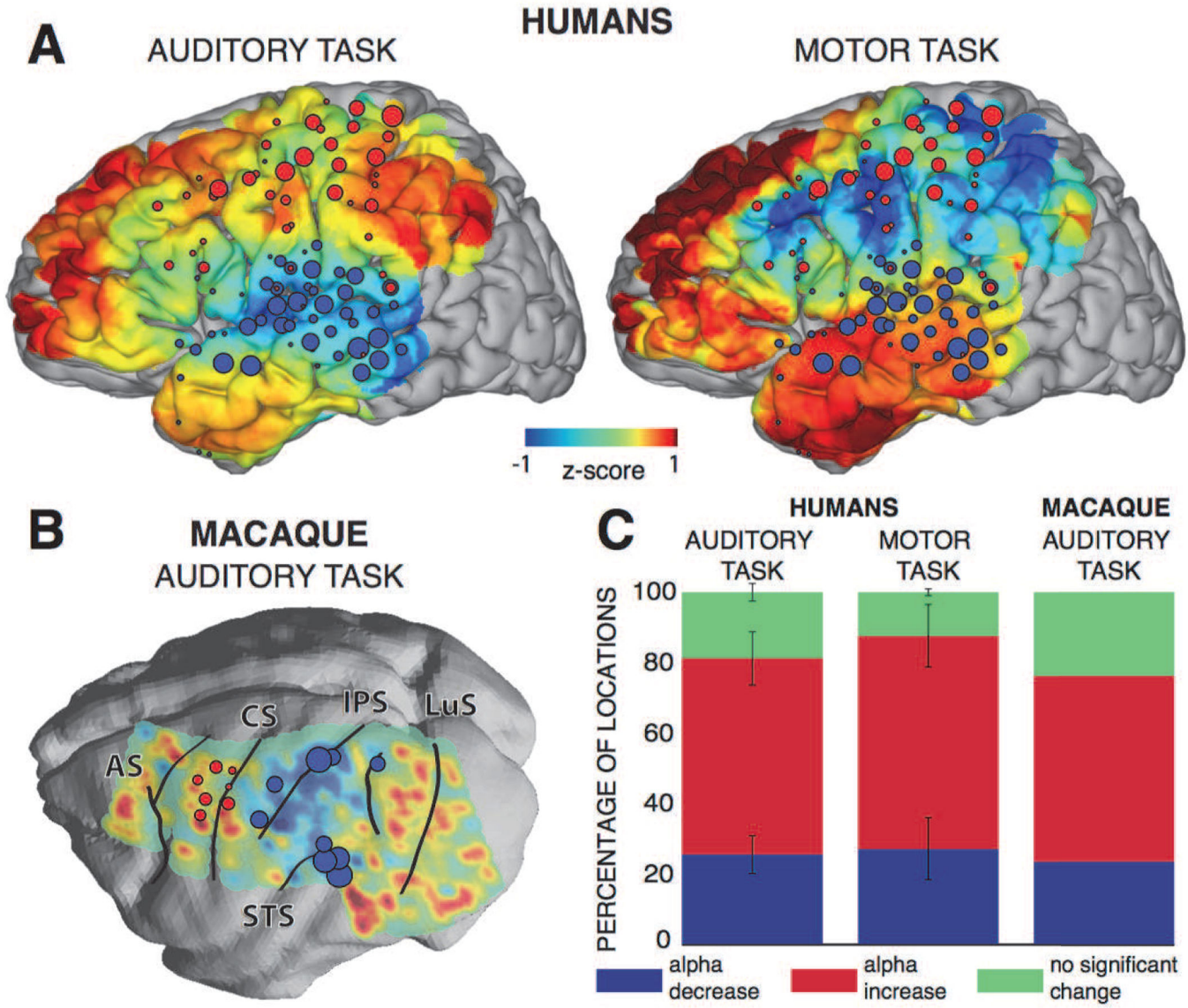

Figure 3. A localized decrease in alpha power in the task-related locations is accompanied by an increase in the majority of the remaining locations

A, B) The topographies show color-coded alpha power averaged during the auditory task for all human subjects (200–800 ms; top left panel) and the macaque (200–800 ms; bottom left panel) and motor task (−300–300 ms; top right panel). Colored circles represent locations that were reactive during the auditory task (blue circles) or the motor task (red circles). AS, arcuate sulcus; CS, central sulcus; IPS, intraparietal sulcus; LuS, lunate sulcus; STS, superior temporal sulcus. **C**) The bar plots show the percentage of all locations for which alpha activity decreased (blue), increased (red) or did not change (green), for the human subjects during the auditory (left) and motor (middle) tasks, and for the macaque during the auditory task (right). Error bars represent the standard error.

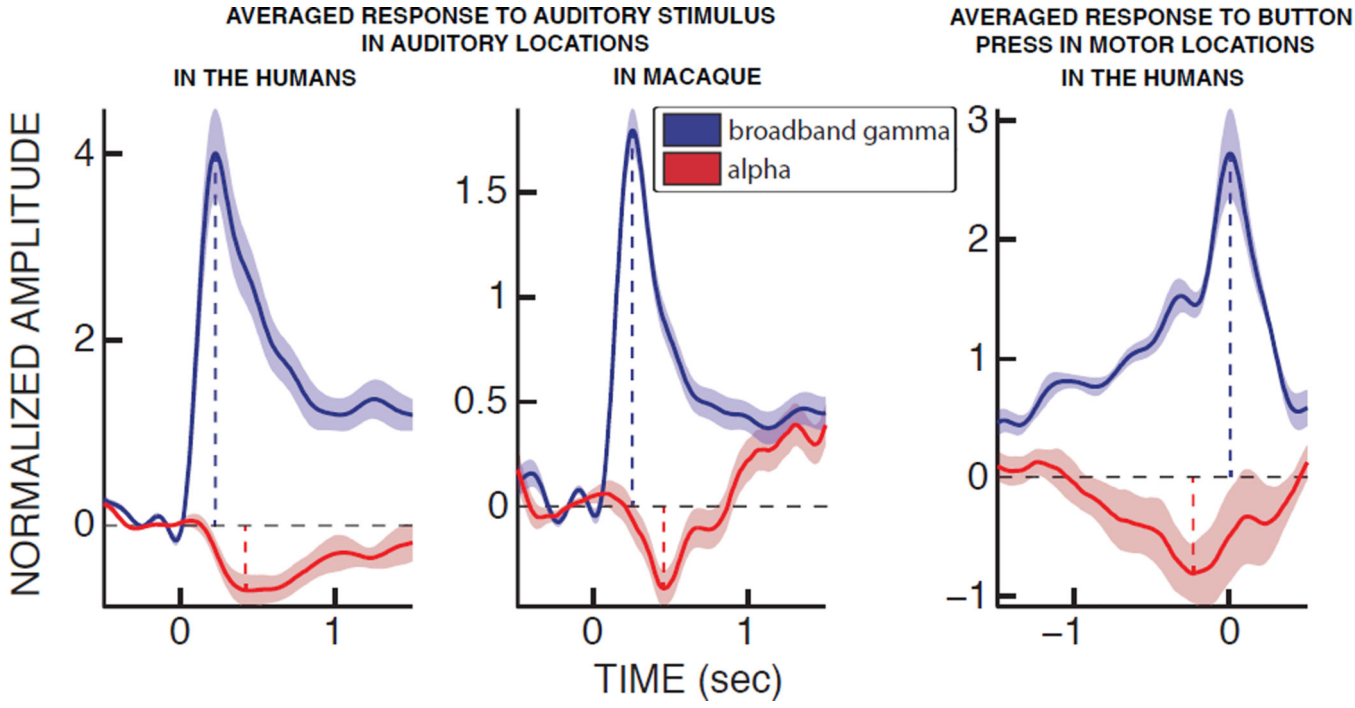

Figure 4. Alpha power suppression lags broadband gamma power in auditory areas during the auditory task, but precedes it in the motor areas during the motor task

The time courses depict the averaged responses in auditory locations during the auditory task in humans (left panel), macaque (middle panel) and in motor locations during the motor task in humans (right panel) for broadband gamma (blue) and alpha (red) bands. Semi-transparent shading represents the standard error. The vertical dashed lines indicate the timing of the positive peaks of the broadband gamma band (blue) and the negative peaks of alpha band (red) for each task.

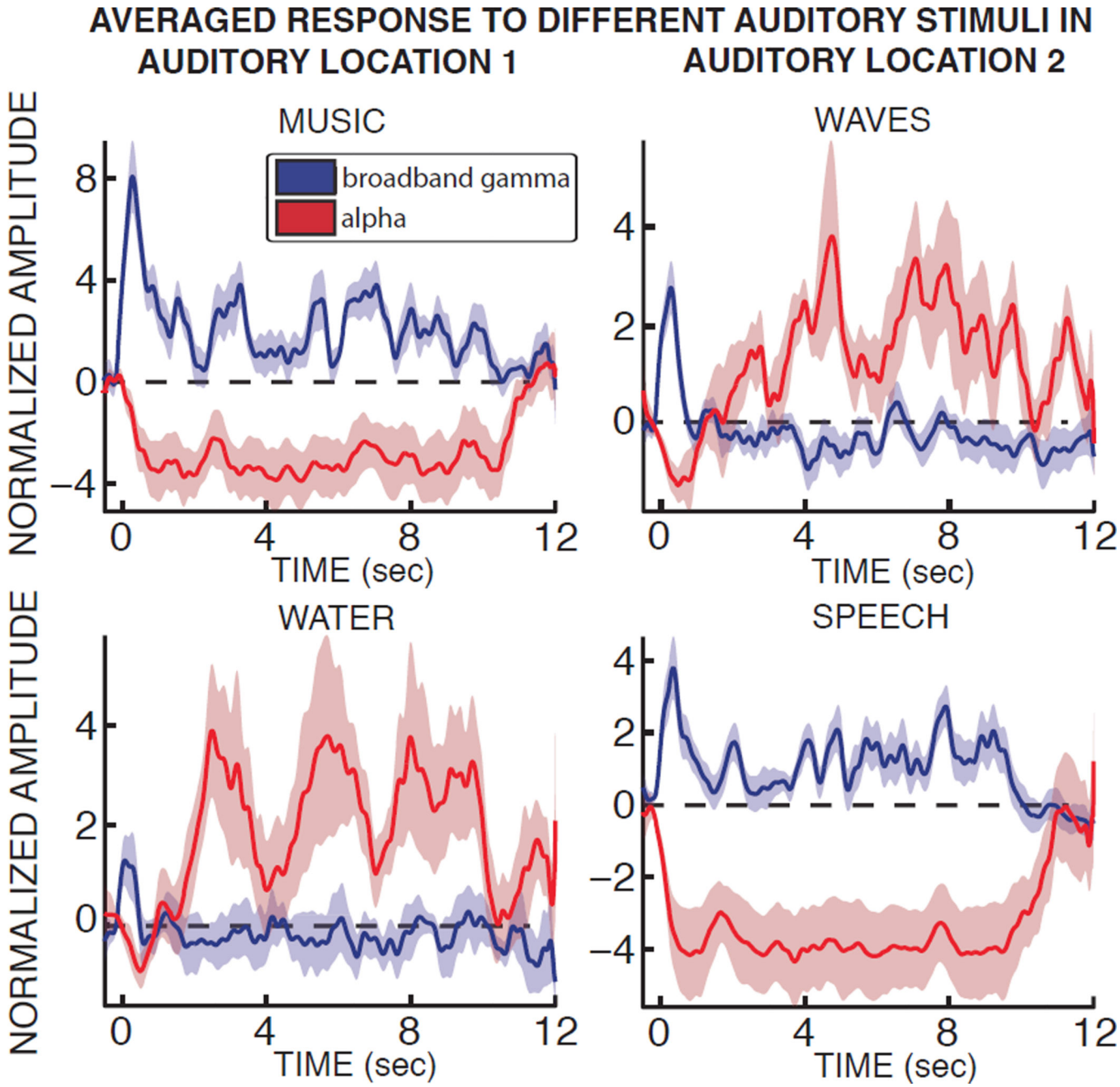

Figure 5. The same auditory location can exhibit drastically different modulations of alpha and broadband gamma power according to the type of auditory stimulus presented

For two different auditory locations in subject A (left and right panels, respectively), the average time courses in response to four different auditory stimuli are shown for alpha and broadband gamma power (red and blue, respectively). Semi-transparent areas represent the standard error.

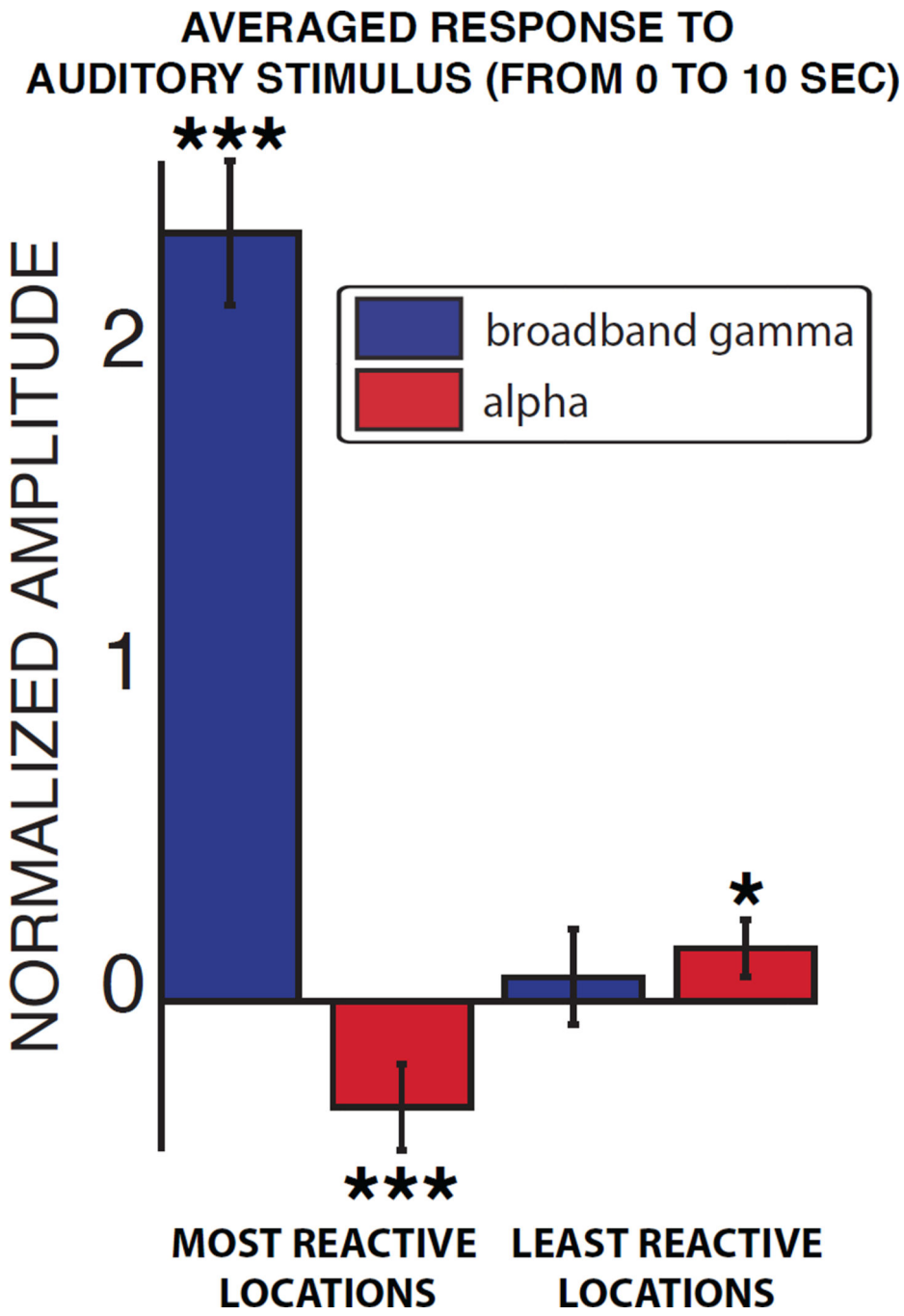

Figure 6. Within the auditory system, patterns of alpha power suppression in reactive locations and increase in non-reactive locations parallel the modulations of alpha power across systems

The bar plots show the amplitude of the responses in broadband gamma (blue) and alpha (red) power, averaged across the most or least reactive locations of the human subjects. Error bars denote the standard error. *: $p < 0.05$; ***: $p < 0.001$.

Table 1

Clinical profiles of the human subjects that participated in the study. All of the subjects had normal cognitive capacity and were functionally independent. Language lateralization (LL) was established using the Wada test.

Subject	Age	Sex	Handedness	LL	Seizure Focus	Grid Locations	# of Elec.
A	29	F	R	L	Left temporal	Left fronto-parietal	64
						Left temporal	23
						Left temporal pole	4
						Left occipital	6
B	36	F	R	L	Right temporal	Right fronto-parietal	40
						Right temporal	35
C	45	M	R	L	Left temporal	Left fronto-temporal	54
						Left temporal pole	4
D	28	M	R	L	Left temporal	Left fronto-parietal	48
						Left parietal	20
						Left temporal	66
						Left frontal pole	4
E	30	M	R	L	Left temporal	Left frontal	40
						Left temporal	35
						Left temporal pole	4
						Left occipital	4